



Internal Report 2012–05

June 2012

Universiteit Leiden

Opleiding Informatica

Optimizing Pedestrian Environments
with
Evolutionary Strategies

Marijn Swenne

Supervisors:

Prof. Dr. Thomas Bäck

Dr. Michael Emmerich

MASTER'S THESIS

Leiden Institute of Advanced Computer Science (LIACS)
Leiden University
Niels Bohrweg 1
2333 CA Leiden
The Netherlands

Abstract

The environment of pedestrians has a big influence on their movement efficiency. Poorly designed environments can lead to high pedestrian densities which in turn increases the risk of injury, or in the case of egress, increases tardiness. A common approach is to have an expert design an environment and test it with a simulator. We propose a method to design a pedestrian environment by using pedestrian simulation in combination with optimization by means of evolutionary strategies. The results demonstrate that thus optimized environment layouts can improve pedestrian throughput in comparison with layouts designed by humans.

Contents

1	Introduction	6
1.1	Related Work	6
1.2	Outline	7
1.3	Research Questions	7
2	Pedestrians	9
2.1	Pedestrian Behaviour	9
2.1.1	Emergent Behaviour	9
2.1.2	Perception	11
2.1.3	Stress	12
2.2	Pathfinding	13
2.2.1	Reduced Visibility Graph	13
2.2.2	Corridor Method	13
2.3	Social Forces Model	14
2.3.1	Steering	15
2.3.2	Static Obstacles	16
2.3.3	Dynamic Obstacles	16
3	Pedestrian Simulation Implementation	17
3.1	Pathfinding	17
3.1.1	Pathfinding Graph Construction	17
3.1.2	Path Selection	18
3.1.3	Attractor Point Selection	20
3.2	Obstacle Avoidance	20
3.2.1	Static Obstacle Avoidance	20
3.2.2	Dynamic Obstacle Avoidance	21
4	Pedestrian Environment Optimization	23
4.1	Pedestrian Density	23
4.2	Evolutionary Strategy	24
4.3	Noise	25

5 Experiments	27
5.1 Simulation Parameters	28
5.2 Simulator Validation	28
5.3 Corridor	29
5.4 Intersection	29
6 Results	31
6.1 Simulator Validation	31
6.2 Environment Optimization	31
6.3 Corridor	32
6.4 Intersection	33
7 Discussion	38
7.1 Simulator	38
7.2 Evolutionary Strategy	38
8 Conclusions	40
8.1 Future research	40
9 Acknowledgements	42
A Emergent Behaviour	43
B Corridor Results	46
C Intersection Results	50

List of Figures

2.1	Lane formation	10
2.2	Circular flows	11
2.3	Clogging effect	11
2.4	Visibility Graph	13
2.5	Corridor Method	14
2.6	Social Forces	15
3.1	Circle Offset	18
3.2	Path creation	18
3.3	Path selection	19
3.4	Congestion Information	19
3.5	Attractor Point Selection	20
3.6	Goffman Scanning	21
4.1	ES evolution	25
5.1	Corridor Setup	30
5.2	Intersection Setup	30
6.1	ES Corridor Run	34
6.2	Corridor Environments	35
6.3	Corridor Efficiency Results	35
6.4	ES Intersection Run	36
6.5	Intersection Environments	37
6.6	Intersection Efficiency Results	37
A.1	Timeseries Lane Formation	43
A.2	Timeseries Circulation Flows	44
A.3	Timeseries Clogging Effect	45
B.1	Corridor Efficiency vs Density per environment	47
B.2	Corridor Efficiency vs Environment per Density	48
B.3	Timeseries Corridor	49
C.1	Intersection Efficiency vs Density per environment	51
C.2	Intersection Efficiency vs Environment per Density	52

C.3 Timeseries Intersection	53
C.4 Timeseries Intersection cont.	54

Chapter 1

Introduction

Pedestrian simulation is a field that has been getting increased attention in the last decade. One of the goals for this field of applied science is to design pedestrian environments for optimal safety and efficiency. We have used a pedestrian simulation in combination with an Evolutionary Strategy to find such environments. This in itself has not been done before and has therefore little related work. However, pedestrian simulators itself is a large field and the following section will therefore begin with a brief overview. Part of the work described in this thesis has also been presented on the 6th International Conference on Pedestrian and Evacuation Dynamics [29].

1.1 Related Work

The two most common models on which pedestrian simulations or crowd simulations are based are the macroscopic and microscopic ones. The macroscopic simulations have been used from the 1970's onwards. In these models, individual movement is not considered and common ways to represent movement and location would be with use of vector fields and density graphs. Although being reasonably accurate on the macroscopic scale, it is not suitable for simulating small scale pedestrian movement. Classic examples of these models are [5] and [4]. The microscopic models became popular from the 1980's onward. In a microscopic model every pedestrian (usually called 'agent') is considered individually. Applying microscopic simulation on a large scale was not computationally feasible in the 1980's, but with advances in computational power, application to large crowds has become more common [13]. Within the microscopic models there are three main categories. The Benefit Cost Cellular Model (BCCM), the Magnetic Force Model (MFM) and the Social Forces Model (SFM). The BCCM was first proposed by Gipps in 1985 [11]. In this model, the space in which agents are placed is represented as a 2D cellular grid. All agents, obstacles and other objects are defined as a cell or a collection of cells. This implies that agent location and movement is discrete in contrast to real world pedestrians

where this is continuous. Other well known examples BCCMs are [19] and [5] The MFM as proposed by [23] is based on each pedestrian, obstacle and goal having a magnetic polarity. The agents and obstacles have positive poles where the agent goals have negative poles. The movement of each agent is the equation of all magnetic fields resulting in agents eventually moving to their goals while avoiding collisions. Finally, the SFM by [17] is very similar to MFM but assumes that repulsion and attraction is a result of social pressures. SFM is currently one of the most commonly used models for pedestrian movement and will be used as a basis for the simulator.

1.2 Outline

The outline of this thesis is as follows. First the research questions are posed in section 1.3. In chapter 2 all relevant pedestrian concepts that are used, rejected or are the source of to derive models are explained. Our pedestrian simulator that is used in the evolutionary strategy is then described in chapter 3. In chapter 4 the evolutionary strategy and how it is used for pedestrian environment optimization is explained. In chapter 5 the experiments are described. After which in chapter 6 the results are presented and discussed in chapter 7. Finally in chapter 8, the research questions are answered and future research presented.

1.3 Research Questions

Goal of this research is to define a realistic pedestrian simulator that serves as a fitness evaluator for an Evolutionary Strategy (ES) optimization in order to maximize pedestrian efficiency.

This leads to the following three research questions:

- Does the pedestrian simulator produce realistic behaviour?

Every optimization based on the simulator stands or falls with the simulators validity. To make sure these results have real world value, agents should display realistic pedestrian behaviour.

- Can the pedestrian simulator be used as a fitness function for an Evolutionary Strategy?

Our fitness function, being the pedestrian simulator is subject to noise. Also, before the experiments, little was known on the robustness of solutions. If the Evolutionary Strategy is to converge, it needs to be able to deal with the noise and solution robustness provided by the pedestrian simulator.

- Can an Evolutionary Strategy find better solutions than human experts?

Slowing down crowds with increasing pedestrian density is significant and unwanted. The most common way to avoid slowdown in pedestrian crowd is to

have a human expert devise the pedestrian surrounding. But can an evolutionary Strategy find a solution that is as good as, or better than solutions devised by human experts?

Chapter 2

Pedestrians

In this section all pedestrian simulation concepts are discussed that are related to the simulator. These concepts form the foundation for the simulator and understanding them is necessary to follow the reasoning provided in 3.

2.1 Pedestrian Behaviour

A pedestrian simulation aims to duplicate individual and collective behaviour of pedestrians. It differs from a crowd simulation where the focus is put on the behaviour of a crowd where-as a pedestrian simulator focuses on the behaviour of individual pedestrians. Our simulator is a pedestrian simulator and therefore need to model behaviour of individual pedestrians as agents.

2.1.1 Emergent Behaviour

Emergent behaviour is behavior of a system that is not explicitly described by the behavior of the components of the system, and is therefore unexpected to a designer or observer. In a pedestrian simulation this would mean any behaviour that is not the result of a conscious decision. A good example is the pedestrian lanes that emerge at pedestrian stream intersections. Pedestrians do not consciously create or are even aware of these lanes.

Pedestrians giving way or any other traffic rules are not considered emergent behaviour since it is the result of a set of rules that are consciously adhered to. In another system this behaviour could be considered emergent, but the simulators perspective is that of the conscious pedestrian; if he consciously made the decision, it is not emergent behaviour.

Following is a description of the emergent behaviour observed among pedestrians [16].

Lane formation: Lane formation occurs when two or more pedestrian streams overlap that do not share the same direction. The effect is most notable

when the overlapping streams are in opposite direction, also known as counter flow. Lane formation refers to the ribbon like pattern pedestrians form while avoiding collisions with other pedestrians. Such ribbons consist of roughly 7-15 pedestrians who walk mostly single file in the same direction. The lifetime of such a ribbon is limited, but increases with pedestrian density. Lane formation occurs readily and can be seen in almost any pedestrian crowd.

Ribbons increase the average speed by reducing the course corrections needed for collision avoidance. The front pedestrian of the ribbon creates a wake in which the rest can follow. A common reason why a ribbon is broken is if it diverges too much from a follower's desired direction. Another cause is followers being cut off by pedestrian walking in opposite direction.

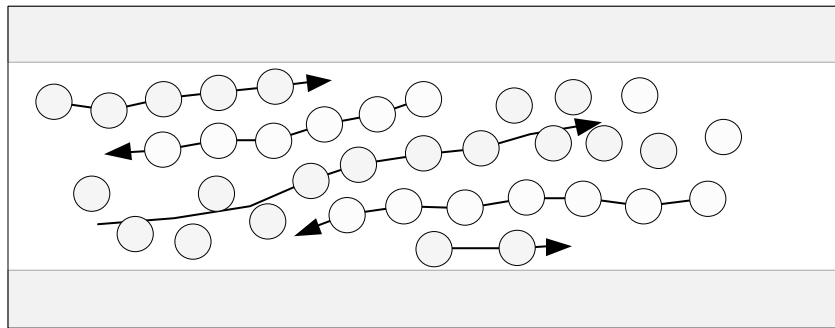


Figure 2.1: Lane formation

Circulation flows: Circulation flows occur at intersections. One such intersection could be two corridors crossing each other in a 90 degree angle where pedestrians arrive from 4 different angles. Circular flows occur in the centre of an intersection with a short lifespan. Occurrences last for a couple of seconds. Duration and frequency are subject to the pedestrian environment and can, for instance, be increased by placing a pillar in the middle of the intersection.

Circulation flows are not more likely to be clockwise than counterclockwise. Also, a previous circulation direction seems to have little predictive value for future circulation directions.

While much less common, it is behaviour like lane formation that makes pedestrian more effective and thus increasing the pedestrian's efficiency.

Clogging effect: The clogging effect occurs before bottlenecks when the amount of pedestrians trying to traverse the bottleneck approaches the maximum capacity. A temporary decrease in pedestrian movement will increase the pedestrian density and in turn decrease pedestrian movement for other pedestrians. The clogging effect is further characterized by an irregular throughput and a radial queue before the bottleneck.

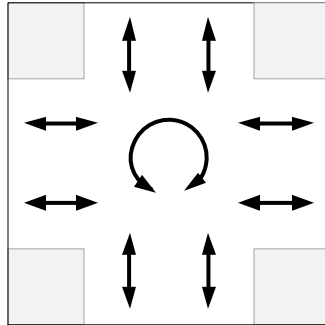


Figure 2.2: Circular flows

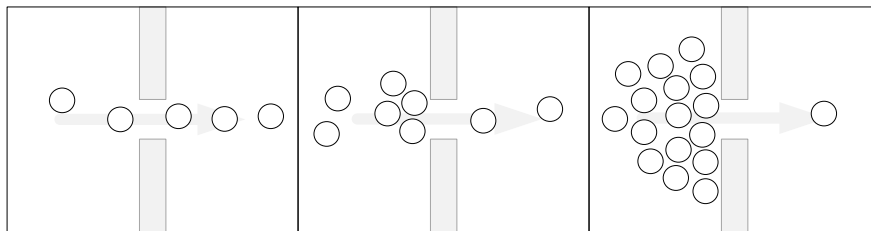


Figure 2.3: Clogging effect

If this clogging effect were to be prevented or delayed, pedestrian efficiency will rise. A valid but maybe extreme example would be to create a single file lane. Since pedestrians cannot be next to each other, clogging as such cannot occur. Research on more subtle changes to the environment to increase pedestrian throughput has been done by Daichi et al. [31]. A pillar was placed in front of the bottleneck where the clogging effect first occurs. The pillar was round and had a diameter of 20 centimeters. Several locations were tried with most resulting in an equal or worse throughput. But with the pillar placed 65 centimeters in front of the exit to the left-hand side, the throughput increased from 2.8 people to 2.92 people per second.

Although such a small increase would be difficult to measure against noise, it does indicate that small and non trivial adjustments in the environment can have a positive influence on pedestrian efficiency.

2.1.2 Perception

Pedestrians observe their surrounding mainly by sight, with hearing and touch playing a smaller role. Goffman, a sociologist, observed pedestrians and came to a model describing how pedestrians take note of their fellow pedestrians and called this process scanning. In this model only a subset of the other pedestrians are influential. If pedestrians are influential is determined by their proximity, radial orientation and if they are separated by other pedestrians. [12]

Pedestrians only take note of what is in front of them and within their influence area. This influence area is in the shape of a halved ellipse stretched in front of the pedestrian. Its size is 2 meters in radius on the minor axis aligned to the width of the pedestrian and with a 5 meter radius on the major axis in front of the pedestrian. Also, other pedestrians will only be of influence if they are in direct line of sight.

2.1.3 Stress

When introducing stress in pedestrian simulation, common associations are the concepts of emergency egress and panic. Emergency egress simulation has been and will be an important application of pedestrian simulation to prevent or reduce injury. Most common scenarios would be emergency evacuation of buildings and passenger vehicles. Many of these egress simulators, or pedestrian simulators used for egress scenarios, integrate the notion of panic. But when looking at the literature, does this model of panic behaviour accurately describe pedestrian behaviour when subject to high levels of stress?

In this model of panic or mass panic, high stress levels will invoke this state and make people act unreasonable and have little or no regard for the well being of themselves or the people around them. The most commonly used examples for panic inducing scenarios are those involving fire, i.e. the emergency egress resulting from a burning building, plane or vehicle. In a pedestrian simulator using this model of panic, the fire scenario is often extended to any scenario with high stress levels.

The notion of mass panic is one that is commonly used in mass media. It is often used as a way of explaining tragic events without having to attribute the cause to a particular person. Even people regarded by the media as experts, such as firemen, refer to the panic model.

In the 1970s, psychologists and sociologists tried to match empirical evidence to this model and found no correlations. Ever since then, there has been a growing scientific movement discarding this model and suspected that a more complex explanation was necessary to elucidate disaster outcomes. This is also true for the field of fire research where it is suggested that the concept of panic does not occur. It is seen as a possible way to blame the outcome of a tragedy on the occupants when in fact the building design or its management were possibly at fault.

In an effort to understand what happens in situations that would previously have been classified as mass panic, Fahy [10] collected evidence by interviewing people who have been in these situations. He concludes that descriptions of ‘panic’ relate more to fear or heightened anxiety than any sort of behaviour leading to the death or injury of a person. Others like Drury [8] have done similar work.

2.2 Pathfinding

In order to circumnavigate obstacles, pathfinding is needed. There are many different pathfinding techniques available for pedestrian simulation and in related fields such as robotic navigation. The following techniques have been used for implementation or inspiration for the pedestrian simulation.

2.2.1 Reduced Visibility Graph

A central geometric structure for calculating the shortest path in applications such as robotic path planning in computer graphics is the visibility graph. This Euclidean graph can be constructed from a collection of polygons by creating an edge between every two polygon corners that are mutually visible. From this, the reduced visibility graph can be derived. The reduced visibility graph G , is constructed as follows. Let a reflex vertex be a polygon vertex for which the interior angle is greater than π . All vertexes of a convex polygon (assuming that no three consecutive vertexes are collinear) are reflex vertexes. The vertexes of G are the reflex vertexes. Edges of G are formed from two different sources:

- Consecutive reflex vertexes: If two reflex vertexes are the endpoints of an edge of $o \in \mathcal{O}$ being all obstacles, then an edge between them is made in G .
- Bitangent edges: If a bitangent line can be drawn through a pair of reflex vertexes, then a corresponding edge is made in G . A bitangent is a line that is tangent to a curve at two distinct points.

Furthermore, these vertexes must be mutually visible from each other. From G a shortest path can be constructed with various algorithms such as the one according to Dijkstra.

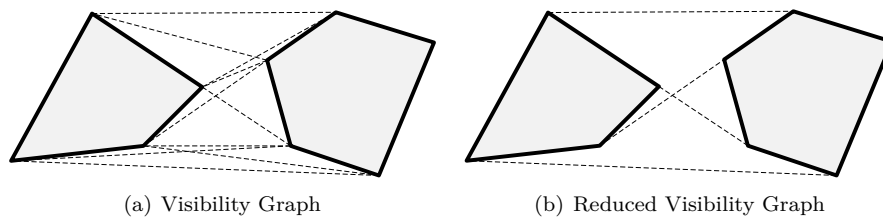


Figure 2.4:

2.2.2 Corridor Method

The Corridor method as described in [18] is a method for guiding an agent through an area or corridor to its desired location. The corridor map is an enhanced graph $G = (V, E)$ whose edges represent collision-free corridors. These

corridors are extracted from the Generalized Voronoi Diagram (GVD) or the environments medial axis.

The GVD or medial axis provide paths between obstacles of greatest clearance. If a path is selected by for instance A^* , A corridor $C = (b_s, r_s)$ can then be defined as a sequence of maximum clearance discs with radii r_s whose center points b_s lie along the backbone path B .

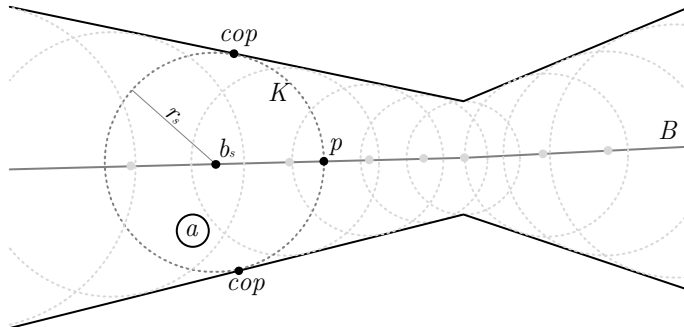


Figure 2.5: Corridor circles for sample point s with backbone path B .

Each sampled point s on the path B is also enhanced with its set of closest obstacle points (cop). This allows us to obtain an explicit representation of the corridors boundary.

Given that an agent a is in such a corridor, an attractor point p can be selected. An attractor point functions as an intermediate goal for the agent, a direction for short termed pathfinding. Attractor point p is determined as follows. Let b_s be the closest sampled point on backbone path B . Let x_a be the current position of the agent. Let b_s denote its corresponding (sampled) point on the backbone path B and $K(b_s, r_s)$ be the largest clearance disc with radius r_s centered at b_s , where $s : s \in [0, 1]$. Then, p can be defined as the furthest point on the agents indicative route $IR \subset B$ that still intersects the boundary ∂K of the clearance disc K . The formula for this is as follows:

$$p_a = IR \left(\underset{s' \in (s, 1]}{\operatorname{argmax}} \{ IR_{s'} \cap \partial K \neq \emptyset \} \right) \quad (2.1)$$

2.3 Social Forces Model

Helbing mentions that the motion of pedestrians can be described as if they were subject to “social forces”. This principal is explored by Helbing [17] who’s model has been shown to reproduce some of the known emergent pedestrian behavior (In particular the Clogging effect and to some degree lane formation). In the following section, the subset of the social forces that will be used in the simulator are described.

The forces, in the Social Forces model, do not translate to physical forces on an agent. Instead they are psychological and drive the agent to move in the direction of the least amount of social pressure. Three different forces can be distinguished; static repulsive forces \vec{f}^s originating from walls, pillars and other immovable obstacles; Dynamic repulsive forces \vec{f}^d originating from other agents and an attractive force \vec{f}^g aimed towards a goal. All forces are represented as vectors which are summed up for each agent to their net social force \vec{f} . An example of each force can be found in Figure 2.3. The Social forces model as described by Helbing also lists attractive forces other than their goal to influence the path of pedestrians such as families that want to stay together. These forces are not used because there is very little known about how these forces work and therefore not contribute to a realistic simulation.

$$\vec{f} = \vec{f}^s + \vec{f}^d + \vec{f}^g \quad (2.2)$$

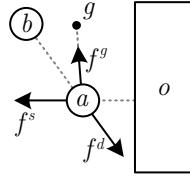


Figure 2.6: Example of the two repulsive forces \vec{f}^s and \vec{f}^d and the attractive goal force \vec{f}^g .

2.3.1 Steering

Let \vec{g}_a^0 be the destination where an agent wants to go. and let the path leading there be a collection of edges $\vec{g}_a^1, \dots, \vec{g}_a^k$. If \vec{g}_a^k is the next edge of this path, the agents desired direction \hat{f}_a^g of motion will be:

$$\hat{f}_a^g := \frac{\vec{g}_a^k - \vec{x}_a}{\|\vec{g}_a^k - \vec{x}_a\|} \quad (2.3)$$

where x_a denotes the position of agent a . The magnitude of \hat{f}_a^g is agents a desired speed v_a , also known as free speed. The steering force of where the agent wants to go is:

$$\vec{f}_a^\gamma = \hat{f}_a^\gamma v_a \quad (2.4)$$

\vec{g}_a^k can also be interpreted as a point with a radius where the next \vec{g}_a^k is selected when the agent is within the radius.

2.3.2 Static Obstacles

Static obstacles are immovably obstacles through which agents cannot pass. Pedestrians become uncomfortable when being close to static obstacles, but only if within 5 meters. As such, a static obstacle o within 5 meters to agent a results in a force on a pointing away from the obstacle. The net static force \vec{f}^s is described as follows:

$$\vec{f}_a^s = - \sum_{o \in \mathcal{O}} \frac{\vec{d}_{ao}}{|\vec{d}_{ao}|} U(|\vec{d}_{ao}|) \quad (2.5)$$

where $\vec{d}_{ao} = (x_o - x_a)\hat{i} + (y_o - y_a)\hat{j}$ being the distance between agent a and static obstacle o . $U(|\vec{d}_{ao}|)$ gives us the magnitude of the repulsive force which is dependent on the distance between agent and the obstacle.

2.3.3 Dynamic Obstacles

Agents are not only influenced by their goal and static obstacles, but also by dynamic obstacles, being other agents. When a pedestrian is close to another pedestrian, they mutually want to increase the distance between them. This is called the territory effect [22] and results in a social force which is represented as \vec{f}^d for an agent. The net dynamic force f_a^d resulting from all other agents present is formulated as follows:

$$f_a^d = - \sum_{b \in \mathcal{A} \wedge b \neq a} \frac{\vec{d}_{ab}}{|\vec{d}_{ab}|} V(|\vec{d}_{ab}|) \quad (2.6)$$

where $\vec{d}_{ao} = (x_b - x_a)\hat{i} + (y_b - y_a)\hat{j}$ being the distance between agents a and b . $V(|\vec{d}_{ao}|)$ gives us the magnitude of the repulsive force which is dependent on the distance between the two agents.

Chapter 3

Pedestrian Simulation Implementation

In this chapter the pedestrian simulator is described. It is based on the concepts and techniques described in the previous chapter and added are the proposition that will be described in the following sections.

3.1 Pathfinding

Pathfinding most commonly refers to the computation of the shortest route between two points. In the simulator, simulated pedestrians do not necessary follow the shortest path. Therefore pathfinding is used to give each agent an indicative route. The indicative route is the shortest path, but the agent will not exactly follow this path but only attracted to it. This is done with use of attractor points or temporary goals that lay on the indicative route and which provide the means for the agent to follow it. How attractor points are selected will be described in the next section. Each agent has one attractor point which defines its preferred direction and consequently the orientation of the vector f^g . The magnitude of f^g is linearly related to the free speed of the agent.

3.1.1 Pathfinding Graph Construction

First a pathfinding graph[21] is constructed on which the shortest path can be calculated with use of Dijkstra's algorithm.

Let there be a collection of obstacles \mathcal{O} placed in environment E . Each obstacle is a convex polygon. Convex polygons are used in order to simplify other calculations. There is no loss in functionality because concave polygon can be build up out of adjacent convex polygons.

Let \mathcal{B} be a collection of obstacle borders, each $b \in \mathcal{B}$ belonging to an obstacle $o \in \mathcal{O}$. b_o is an extension of polygon o by range r , drawing a region of constant width around o . A common value for r is the radius of an agent. See 3.1.1

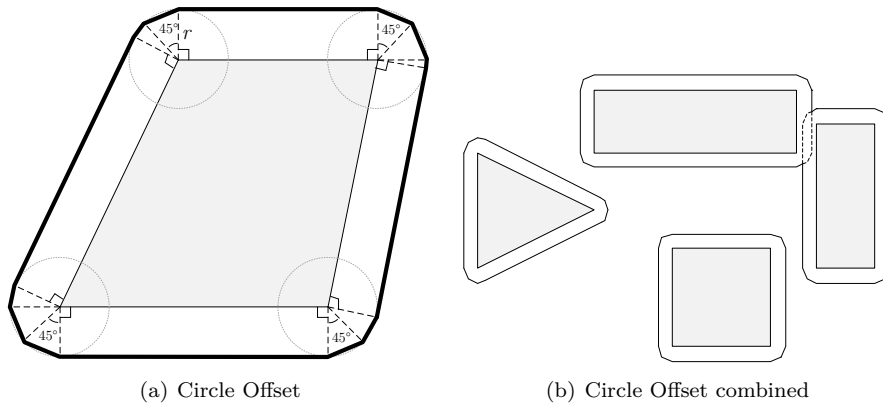


Figure 3.1:

If two obstacle borders are overlapping, the overlapping edges are broken at the point where they intersect. All edges that are enclosed are discarded with the remaining edges forming a new obstacle border, replacing the original two. See 3.1(b). G is constructed by creating a reduced visibility graph from the polygons contained in \mathcal{B} .

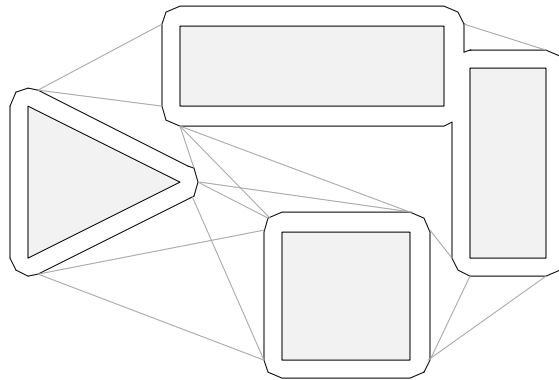


Figure 3.2: Path creation

A Euclidean graph G is constructed by creating a reduced visibility graph from the polygons contained in B . This will result in a graph as shown in 3.1.1.

3.1.2 Path Selection

When calculating a route, it is the expected travel time that determines the shortest path. Dijkstra's algorithm is used to determine the shortest path P over graph G . To determine this, every edge of G has a speed attributed, being the average speed of agents that walk over that edge. An Agent is considered

to be walking over an edge if the circle representing the agent overlaps with the edge.

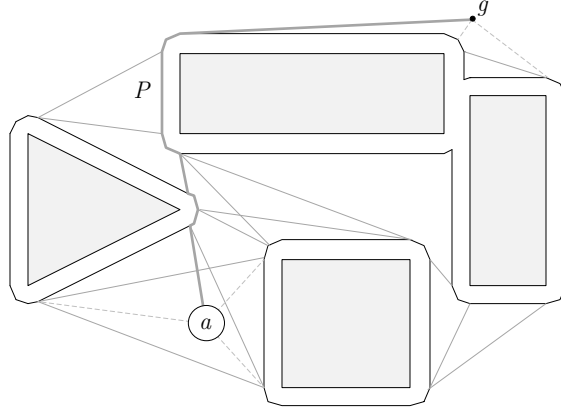


Figure 3.3: Path selection

Every agent has an individual freespeed. The time it will take to complete a path will therefore vary amongst agents. The estimated travel time for an edge is determined by dividing the edge's length by the average speed of the agents on that edge. However, if the edge's average speed is higher than the agent's freespeed, the edge length is divided by the agent's freespeed.

Note that agents with a lower freespeed are less hindered by congestion and need a higher congestion rate before choosing a detour.

As noted by [32], when congestion increases there is an increased chance of recalculating the route for a possible faster alternative.

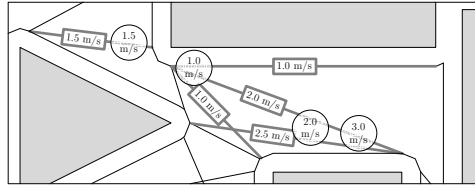


Figure 3.4: Congestion Information

The chance an agent has for recalculating their route is dependent on the time since the last (re)calculation t , current speed w_a and free speed v_a .

$$\frac{1}{(1 + e^{ct}) / (1 + h \frac{w_a}{v_a})} \quad (3.1)$$

Where c influence the shape of the curve and h is a scalar increasing or decreasing the chance. For the simulator $c = -0.002$ and $h = 99$ are used.

3.1.3 Attractor Point Selection

The attractor point p is the point that will be used to determine the steering direction for agent a (\vec{f}_a^g) in the social forces model.

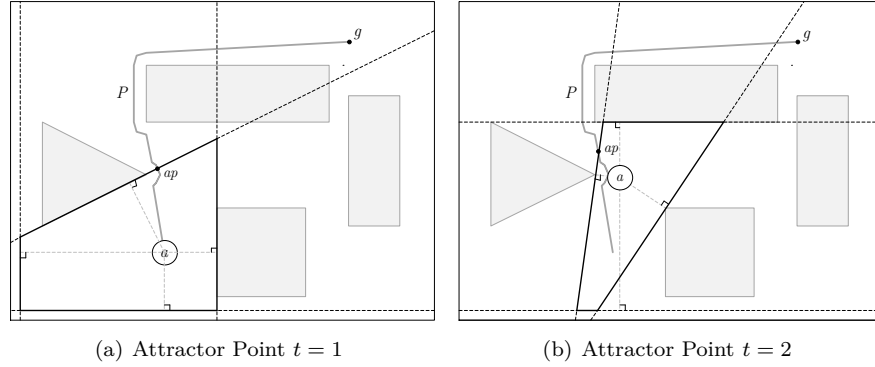


Figure 3.5:

Let T_a be a collection of all tangent lines on obstacles \mathcal{O} that have a 90 degree angle with agent a and let T'_a be the collection of line segments resulting from breaking each line from T_a where they are overlapping. Attractor region R_a is a polygon constructed from all line segments in T'_a that are in direct line of sight of a and not obstructed by other line segments from T'_a . ap_a is the point where the border of R_a cuts P_a or p_a^0 if no such point exists. See Figure 3.5(a),3.5(b).

3.2 Obstacle Avoidance

In this section the implementation the avoidance of both static and dynamic obstacle avoidance are covered.

3.2.1 Static Obstacle Avoidance

Static obstacle avoidance involves all course corrections an agent makes to try to avoid collisions and keep distance between itself and any non-agent obstacles i.e. walls and pillars. The technique suggested by the social forces was employed without any further adjustments. The function $U(|\vec{d}_{ao}|)$ was implemented for determining the magnitude of \vec{f}^s as follows:

$$U(|\vec{d}_{ao}|) = \frac{m_a + r_a - |\vec{d}_{ao}|}{(|\vec{d}_{ao}| - r_a)^2} \quad (3.2)$$

Where r_a is the radius and m_a the Goffman eclipse distance of a .

3.2.2 Dynamic Obstacle Avoidance

Dynamic obstacle avoidance involves all course corrections an agent makes to try to avoid collisions and keep distance between itself and other agents. Pedestrians are known to be very adept in avoiding collisions with other pedestrians, even in high density crowds. Also, while avoiding collisions, the lane formation and circular flow behaviour starts to emerge. One of the criteria on which the simulator should be tested is therefore how well dynamic obstacle avoidance resembles real world scenarios. Unfortunately data on this subject is not readily available and time consuming to acquire. It is therefore important to note that observing these phenomena is essential to validate a simulator, but having a higher rate of occurrences of these phenomena does not equate to a better simulator. Ondrej et al. [24] for instance proposes a collision avoidance model based on vision and collision prediction. He notes that Helbing's social forces model shows very little to no lane formation in dense crowd. His more complex model is very adept in forming lanes. So much so, that it supersedes the abilities of the average pedestrian. We have therefore strived for a dynamic obstacle avoidance model in which lane formation and circular flows emerge, but with the least amount of complexity and rules that can be derived from pedestrian observations instead of rules to directly stimulate emergent behaviour. Since lane formation and circular flows are emergent behaviour in pedestrian crowd, they should also emerge in the simulator as opposed to being forced to appear.

Our model is mainly based on the social forces model where a dynamic obstacle causes a repulsive force if they are present in the pedestrians influence area. To calculate the net force, all other agents have to be observed and have them project vectors on the agent representing social forces, pushing the agent away from the dynamic obstacles. The magnitude is related to the distance between the agent and obstacle. This creates some of the emergent behaviour seen in pedestrians[15]. A second set of rules based on Goffman's research[12] was added on how pedestrians observe and prioritize other pedestrians. This addition gives us a model that is more lifelike and shows better lane formation in dense streams. In 3.2.2 a visual representation is given on which agents exert influence with the grey agents being excluded.

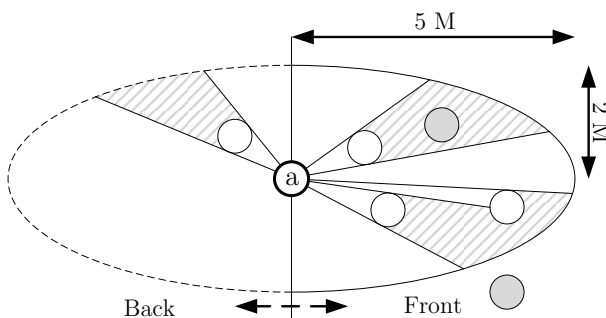


Figure 3.6: Goffman Scanning

Every dynamic obstacle that influences the agent results in \vec{d}_{ab} which is a repulsion vector starting at a pointing away from b . The calculations used for \vec{f}^d given by the social forces model are employed. The additions suggested above are implemented by only having agents influence other agents if they are scanned and by implementing $V(|\vec{d}_{ab}|)$ which determines the magnitude of the force as follows:

$$V(|\vec{d}_{ab}|) = |\vec{d}_{ab}|^{-2} * \frac{L(a, b)}{L(a, min)} \quad (3.3)$$

Where $L(a, b)$ is the length from a to the ellipse at angle \hat{d}_{ab} , and $L(a, min)$ being the length from a to the ellipse on its minor axis.

Chapter 4

Pedestrian Environment Optimization

In the previous chapter the pedestrian simulator functions was described. In this chapter it is explained how this simulator is used for pedestrian environment optimization and how optimization takes place.

A pedestrian environment is a collection of obstacles represented as polygons. Optimizing this means moving and/or reshaping these obstacles to maximize efficiency. For every such obstacle, these operations can be bounded. Representing the pedestrian environment in this way makes for a real valued, multidimensional search space. Heuristics is used to try and find the most desirable environment. Heuristics does not warrant the best environment is found (even if the best environment would be found, there is no way of checking that it actually is the best), but given the search space, is the best option for finding good solutions in reasonable time.

4.1 Pedestrian Density

Pedestrian efficiency is largely a function of the environment and pedestrian density. It can also be stated that the throughput of an environment (how many pedestrians can traverse the environment given a time frame) is the product of the pedestrian density and the pedestrian efficiency.

When pedestrian density increases, efficiency eventually drops. However, when and how much this drops is partially dependent on the environment. When looking at it from this perspective, optimizing pedestrian efficiency is reducing the negative effect that density has on efficiency.

Because the negative effect is insignificant at low densities, optimization should occur at high densities, increasing the possible net gain in efficiency (When starting at 99%, there is only a possible net gain of 1%). Because high density is not a well defined term, several densities should be explored.

4.2 Evolutionary Strategy

An Evolutionary Strategy (ES) belongs to a group of metaheuristic optimization algorithms called Evolutionary Algorithms (EA). An EA optimizes with use of mechanics inspired by biological evolution being: reproduction, mutation, recombination and selection. It works well in the real-valued domain. It is also developed and most commonly used for Euclidean search spaces which makes it very suitable to optimize a pedestrian environment.

Overview: To try and find the best solution (highest or lowest fitness), a collection of solutions (children, which collectively are referred to as a population) is created after which the fitness of each member is determined. Now a cycle or generation is repeated until a stopping criteria is satisfied. First, one or more parents are selected most commonly based on fitness. From those parents new solutions or children are created with use of recombination and/or mutation. These children from the new population which is then evaluated completing the cycle. The most common criteria to stop this cycle are time, convergence velocity and a solutions fitness crossing a threshold.

```

Initialization
Evaluation
while (not stopped){
    Selection
    Recombination and Mutation
    Evaluation
}

```

A more formal definition of this archetype ES as noted in [2] takes the following form. An individual a consisting of an element $X \in R^n$ is mutated by adding a normally distributed random vector $Z_t \tilde{N}(0, I_n)$ that is multiplied by a scalar $\sigma > 0$. I_n denotes the unit matrix with rank n . The new point is accepted if it is better than or equal to the old one, otherwise the old point passes to the next iteration. The selection decision is based on a comparison of the objective function values of the old and the new point. Assuming that the objective function $f : R^n \rightarrow R$ is to be minimized, the simple ES, starting at some point $X_0 \in R^n$, is determined by the following iterative scheme:

$$X_{t+1} = \begin{cases} X_t + \sigma_t Z_t & \text{if } f(X_t + \sigma_t Z_t) < f(X_t), \\ X_t & \text{otherwise.} \end{cases} \quad (4.1)$$

Mutation: A (1,10)-ES with one scalar σ , more commonly referred to as stepsize, per solution is used. For this variation, recombination is not applicable and mutation is as follows: an individual $\vec{a}((x_1, \dots, x_n), \sigma)$ consisting of elements X and stepsize σ is mutated by first determining the new stepsize $\sigma' = \sigma \exp(\tau_0 \cdot N(0, 1))$ with τ_0 being the learning rate and $N(0, 1)$ a normal distribution centered on 0 with a standard deviation of 1. The new stepsize σ' is

then used for determining the new values for X' as follows: $x'_i = x_i + \sigma' \cdot N_i(0, 1)$ which results in the mutated individual $\vec{a}'((x'_1, \dots, x'_n), \sigma')$. The learning rate τ_0 defines how fast the ES tends to converge. A common value is $\tau_0 = 1/\sqrt{\lambda}$.

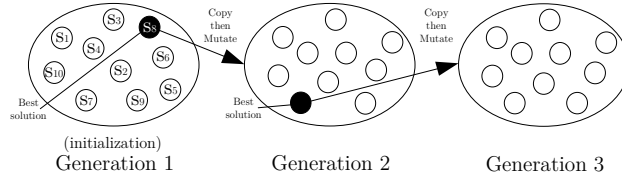


Figure 4.1: Evolution of a (1, 10)-ES where black represents the best solution

Notation: The notation convention for the amount of children and parents used in an ES is as follows: (μ, λ) -ES or $(\mu + \lambda)$ -ES. The $+$ means that the parents are able to be part of the new generation whereas the $,$ means that only children from the selected parents are to be selected for the next generation. μ is the amount of parents selected for reproduction and λ is the population size. If only one parent is used for reproduction it is a $(1, \lambda)$ -ES or $(1 + \lambda)$ -ES.

4.3 Noise

One of the main issues to use the simulator as fitness function for the ES is noise. The cause is the pseudo random number generator used for agent movement. This means that running the fitness function on a solution more than once will result in fitness values that are different. Also, solutions that are similar in genes are significantly less similar in fitness values indicating a noisy fitness landscape or a solution that is not robust. For quantitative evidence, please see 6.

There are four different pseudo random number generators that contribute to the noisy fitness function. The first two determine the starting location of agents and when a pedestrian recalculates its route. These both generate uniform distributed values. The last two determine the agent's free speed and the agent's stepsize (not to be confused with the mutation stepsize regarding the ES). Both generate Gaussian distributed values.

To make the ES more robust, techniques for noise reduction are employed as described by Krusselbrink [20] in particular resampling. The fitness of a solution is then described as then average fitness over m samples and can be noted as follows:

$$\hat{f}_{\text{exp}}(x) = \frac{1}{m} \sum_{i=1}^m \tilde{f}(x) \quad (4.2)$$

Where \hat{f}_{exp} is the expected fitness function. This increases the function evaluation by factor m . Given that the best solution is sought within a given

evaluation budget (the amount of fitness evaluations allowed), it is important to explore alternative ways to spend these fitness evaluations. One way is to increase the number of generation by factor m . This only has a significant effect if the ES does not converge. Another more common alternative is to increase the amount of children in a generation by factor m . This works well for a CMA-ES [14] which is a variation of an ES which is briefly touched upon in 8.1. However, for a (μ, λ) -ES, the resampling technique works best. And since the selected $(1, \lambda)$ -ES is a simple version of the (μ, λ) -ES the resampling technique will be employed.

Another issue is determining a value for m . Several tests have been conducted by Kruisselbrink for a $(\mu/2_{DI}, \lambda) - \sigma SA$ -ES with $\mu = 5$ and $\lambda = 35$. These show that setting m to 1 or 10 produces similar results, but setting m to 5 produces better results. Given these results and the fitness evaluation budget, m has been set to 3.

Chapter 5

Experiments

Three experiments are devised. The first is simulator validation in order to understand how well the simulator reproduces pedestrian behaviour. The second two, called the Corridor and Intersection experiments, test if the Evolutionary Strategy can use the simulator as a fitness function, and the quality of the solutions. One of the research questions is if an Evolutionary Strategy can find a better environment than an expert. To test this, we have taken on the role of environment experts and designed 3 environments for each of the second two experiments. A render of these solutions can be found in 6.3,6.4.

For both the Corridor and Intersection experiment the fitness of the 3 expert environments to the 3 best environments found by the ES are compared. As stated in 4.3, resampling is used to assess the fitness of each environment. During an ES run, $m = 3$ will be used. In an attempt to further reduce the noise and get a more accurate reading, $m = 50$ is used for comparing the 3 expert and 3 ES environments. Every environment will also be tested for different agent spawn frequencies. The frequencies range from 0.2, there being hardly any agent interaction, to 100, where congestion commonly occurs.

The Corridor and Intersection experiments produce solutions or environments that represent geometric setups. Each setup consist out of agent starting zones, each with a corresponding goal and a collection of static obstacles O . Agents are spawned in their starting zones and will attempt to find a route to their goal. When an agent reaches its goal area, he will be removed. In this context maximizing pedestrian efficiency means minimizing the average time between agents being spawned and removed. As noted by [3], Social forces models are well suited for measuring mean pedestrian walking times. Efficiency is measured in percentages where 100% equals the mean time agents need to complete their route if there are no static or dynamic obstacles.

Each agent has a freespeed parameter that determines its maximum velocity. These are distributed among the agents spawned as they are distributed among a general pedestrian population as noted by [7]

Experiments are run on a desktop computer that possess 8 cores. Running the fitness function for of each child occurs in parallel. All experiments have 10

children and because running the fitness function takes up the majority of the time, all available CPU resources are used.

5.1 Simulation Parameters

When using the simulator for producing a fitness value given an environment, some parameters need to be set that haven't been addressed previously. Following is a listing of these parameters, their implications and the values that are used.

Agent spawn frequency: How often an agent is added or spawned at every starting location per second given that this place is not obstructed by another agent. A higher spawn frequency most often results in a higher pedestrian density. However, if no available space can be found, no agent is spawned. This means there is a limit to the frequency at which agents can spawn. If this limit is exceeded, the effective spawning frequency will be lower than the desired spawning frequency. For comparing environments in the results section different spawn frequencies are used, but during optimization, a spawning frequency of 100Hz has always been used, achieving an effective spawning rate close to the maximum possible in the environments tested.

Timeout: A timeout window is imposed on every function evaluation. When an environment is very inefficient, the cost to find out exactly how inefficient it is, is better spent evaluating additional environments (given that this takes a lot of computational resources). If during a fitness evaluation the simulator has simulated 300 seconds without all agents having reached their goals, the simulation is halted with all remaining agents being attributed the maximum time of 300 seconds for reaching their goal.

Agents per simulation: This is the total amount of agents that are spawned during the simulation. A large number of agents spawned in combination with a high spawning frequency cause a high agent density. Because of limited resources, this value has been set to 100 for every simulation.

Calculations per second: Time for pedestrians is for all purposes continuous. However, the simulator can only process the movement of pedestrian in a discrete fashion. To that purpose time is quantized in 10 ms intervals, hence the simulation algorithm was iterated 100 times per second.

5.2 Simulator Validation

To validate a pedestrian simulator one would ideally have metric data on pedestrians and together with expectations derived from this data validate the simulator. There has been some research on generalizing pedestrian movement from

actual captured pedestrian data [28, 6], but despite these efforts it is still not feasible to validate any pedestrian model on the basis of this data. There is an increasing demand for this kind of research [1] and should be the future way to validate pedestrian models.

A more commonly applied approach is to validate a pedestrian simulator by the emergent behaviour it produces. Using emergent behaviour as a validator is based on the premise that a simulator showing the same emergent behaviour as the simulated system confirms the validity of the simulator. Although commonly applied, this premise does not seem very plausible. The opposite however, is more plausible. If a simulator does not show emergent behaviour, it is unlikely to be a valid simulator. A real time representation of a pedestrian simulation will therefore be observed while noting the similarities and dissimilarities between the pedestrian and agent behaviour, further illustrating this with some examples.

For every kind of emergent behaviour described in 2.1.1 an environment has been created that should have them occur if used by real pedestrians, Timeseries from these experiments can be found in A. Although as previously mentioned, there are known limitation in this form of validation, it is necessary given the time constraint of this project and the current state of this research field.

5.3 Corridor

Before running this experiment it was assumed that an empty corridor with no obstacles would be a candidate for the most efficient corridor. To give the optimizer the opportunity to converge on this solution, the obstacles have a variable size, allowing to create a solution very similar to that of an empty corridor.

Following is a description of the environment that is optimized in the corridor experiment. The corridor setup shown in Figure 5.3 (left) has agents starting in areas Z and X with the goal of the agents spawning in area Z to reach area X , and vice versa. Alongside the corridor in between areas Z and X are five static obstacles a, b, c, d, e . These obstacles are square pillars that can be moved along the width of the corridor (denoted by the dotted line) and changed in radius r . An agent cannot intersect with the corridor wall and the only possible route from the agents starting area to their goal is through the corridor.

Each obstacle is represented for the evolutionary strategy by two real valued dimensions, one representing the position along the width of the corridor and the second one representing the obstacle's radius.

5.4 Intersection

The intersection experiment was designed in parallel to the corridor experiment. In this scenario the optimizer attempts to find locations for obstacles of a fixed size such that pedestrians are hindered in the least possible amount.

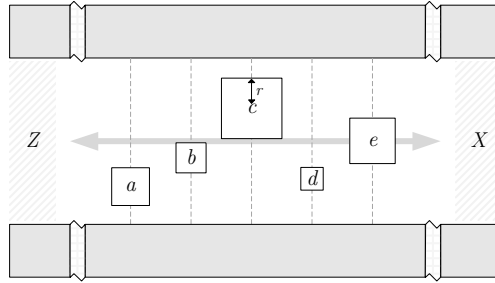


Figure 5.1: Corridor Setup

Following is a description of the environment that is optimized in the intersection experiment. The intersection setup in Figure 5.4 (right) consists of two corridors intersecting in a 90 degree angle with the overlapping, traversable part of the two corridors being area K . The starting areas where the agents spawn are W, X, Y and Z . The goal area for the agents that spawn in W is Y , for Y it is W , for X it is Z and for Z it is X .

In area K , four square static obstacles a, b, c, d of identical size are placed. They can be moved to any place within K while not overlapping the border of K and not overlapping any of the other obstacles.

Each obstacle is represented for the evolutionary strategy by two real valued dimensions, being the x and y position of the obstacle in the intersection.

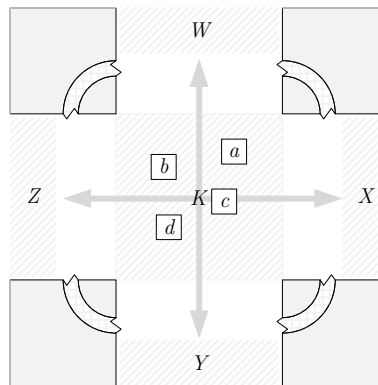


Figure 5.2: Intersection Setup

Chapter 6

Results

In this section the results of the experiments described in 5 are presented. First the validation results of the simulator are presented after which the experiments for finding optimal pedestrian environments are presented.

6.1 Simulator Validation

Overall, the same emergent behaviour in the simulator as amongst real-life pedestrians could be observed, although some behaviour resembled real-life pedestrians more profound than others.

Lane Formation: Lane formation occurs as described in 2.1.1. Lanes form readily and have limited lifespan. The length is also limited to 10-20 agents. When lane formation does not occur, efficiency is, as expected, greatly reduced. A timeseries illustrating these results can be found in the appendix in A.

Circulation Flows: Circulation flows do not seem to occur. Although an unbalance in direction can be seen at some points in time, it's not quite a circular flow. It seems that half of a circle is created, but is then disrupted. A timeseries illustrating these results can be found in the appendix in A.

Clogging Effect: The clogging effect presents itself at agent bottlenecks. The shape resembles what is described by observational studies and efficiency is also decreased. A timeseries illustrating these results can be found in the appendix in A.

6.2 Environment Optimization

In this section the findings for both the Corridor and Intersection experiments are presented. First it is shown how well the simulator is suited as a fitness

	0.2	0.4	0.6	1	2	4	100
Empty	94,38	93,42	89,19	86,77	82,24	72,80	67,75
Middle 2/3	89,53	85,04	81,71	77,21	74,02	69,33	66,47
Middle Centre	90,61	86,78	83,71	79,91	71,50	62,74	58,87
ES I1	88,27	84,34	80,85	80,40	77,77	76,32	69,52
ES I2	89,17	83,29	78,09	79,73	72,28	70,31	75,62
ES I3	89,73	85,27	80,26	75,80	72,07	71,78	68,99

Table 6.1: Percentages of pedestrian efficiency at various spawn frequencies for 3 expert environments and 3 environments found by the Evolutionary Strategy for the Corridor experiment

evaluator for the evolutionary strategy. After which the comparisons in agent efficiency between the environments found by the ES and the expert environments are shown.

6.3 Corridor

Three runs were executed. The stop condition for optimization runs is based on an internal convergence measure of the solution set maintained by the optimizer. In terms of computational effort, the average completion time per optimization run is about one day. In every run convergence was achieved although the generation at which this occurred differed. An illustration on how these runs developed can be seen in Figure 6.3. Note that the fitness values used by the optimizer is the average number of calculation steps needed for an agent between spawning and reaching its goal. The best solution found in each run, i.e., the solution with the best fitness, is used as a representative. Best solutions are designated with a C, e.g., the best solution from the second corridor run is labeled C2. A visual representation of these 3 ES solutions together with the 3 expert solutions can be seen in Figure 6.3

For each environment and spawn frequency¹, fifty simulations have been performed, and the average performance is measured. The Kolmogorov-Smirnov test indicates that each collection is very unlikely to be normally distributed $p < 0.05$. The results are presented as a percentage of the agent potential. An agent’s potential is the time taken from start to goal if no obstacles are present, being 32.35 seconds. All results are summarized in Figure 6.3, showing how the fixed and the optimized environment’s geometry efficiency changes with increasing spawn frequency. For large spawn frequency, optimization can clearly increase efficiency.

Further breakdown of the data in box plots can be found in Appendix C. Also, timeseries examples of fitness evaluations for each of the 6 environments have been included in Appendix B

¹Spawn frequency, in Hz, refers to how often agents are added to a starting area.

	0.2	0.4	0.6	1	2	4	100
Middle Cluster	91,35	79,72	69,01	57,64	49,53	49,59	51,17
Corners	93,99	85,73	72,89	60,14	48,08	45,39	44,56
Side Middle	91,83	82,10	72,48	61,20	52,31	49,86	47,39
ES 1	88,48	78,99	65,87	59,74	50,91	43,39	45,28
ES 2	88,94	78,67	68,26	59,76	51,93	50,91	49,21
ES 3	90,82	80,95	69,37	62,48	56,09	50,32	48,70

Table 6.2: Percentages of pedestrian efficiency at various spawn frequencies for 3 expert environments and 3 environments found by the Evolutionary Strategy for the intersection experiment

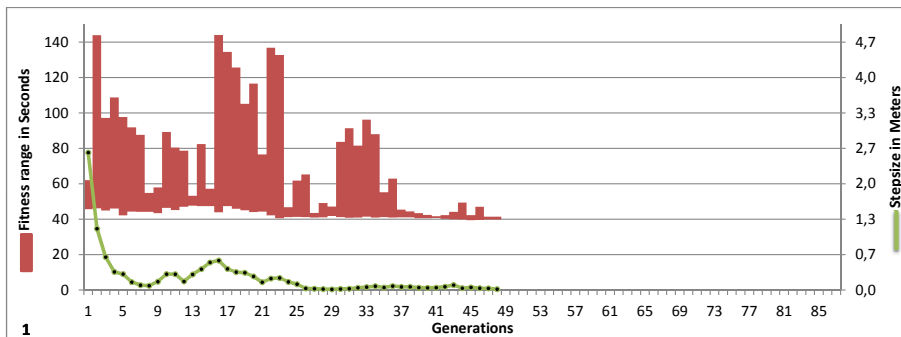
6.4 Intersection

Three runs were executed. The stop condition for optimization runs is based on an internal convergence measure of the solution set maintained by the optimizer. In terms of computational effort, the average completion time per optimization run is about two days. It is not clear if convergence took place although the stepsize did decrease. An illustration on how these runs developed can be seen in 6.4. Note that the fitness values used by the optimizer is the average number of calculation steps needed for an agent between spawning and reaching its goal. The best solution found in each run, i.e., the solution with the best fitness, is used as a representative. Best solutions are designated with an 'I', e.g., the best solution from the second corridor run is labeled I2. A visual representation of these together with the 3 expert solutions can be seen in 6.4

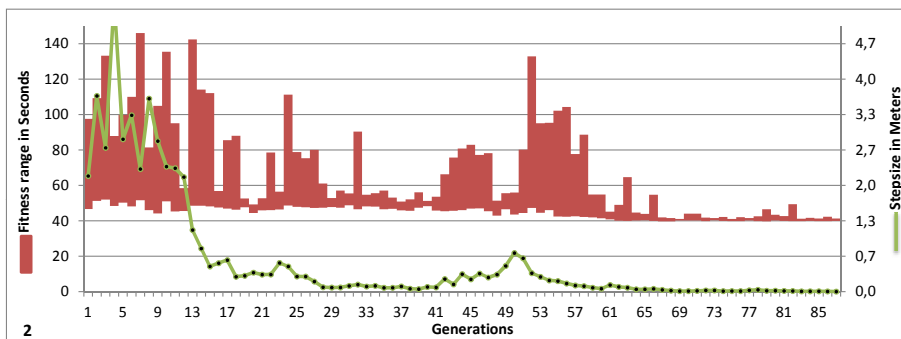
For each environment and spawn frequency², fifty simulations are performed, and the average performance is measured. The Kolmogorov-Smirnov test indicates that each collection is very unlikely to be normally distributed $p < 0.03$. The results are presented as a percentage of the agent potential. An agent's potential is the time taken from start to goal if no obstacles are present, being 19.08 seconds. All results are summarized in Figure 6.3.

Further breakdown of the data in box plots can be found in B. Also, time-series examples of fitness evaluations for each of the 6 environments has been included in Appendix C

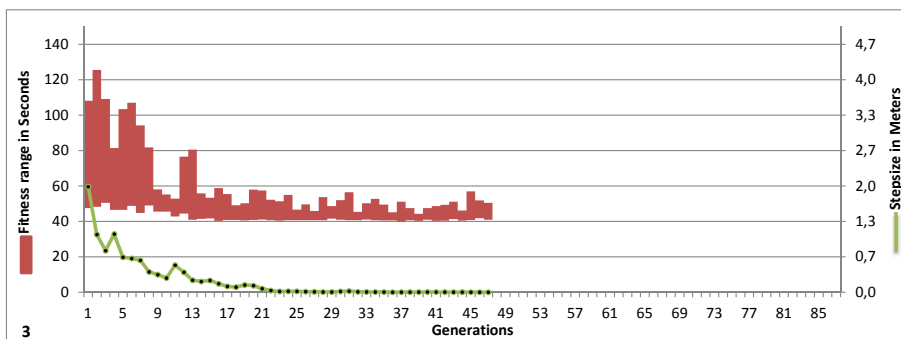
²Spawn frequency, in Hz, refers to how often agents are added to a starting area.



(a) ES C1



(b) ES C2



(c) ES C3

Figure 6.1: Progression of Evolutionary strategy for the Corridor experiment. Pedestrian range is from the child with the best fitness to the child with the worst fitness of that generation.

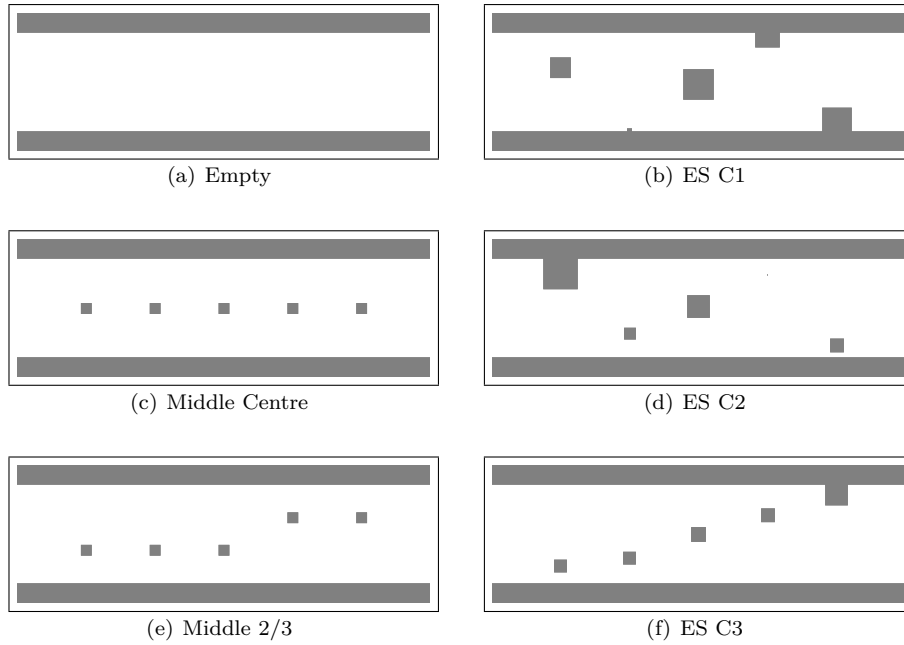


Figure 6.2: Visual representation of the 3 expert Corridor environments on the left and 3 environments found by the Evolutionary Strategy on the right

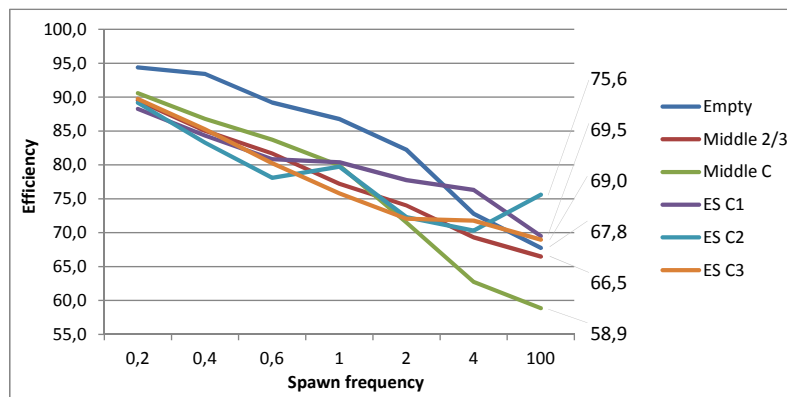
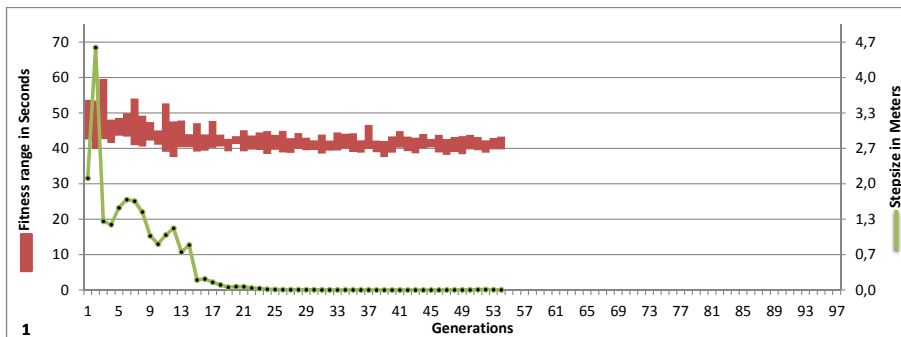
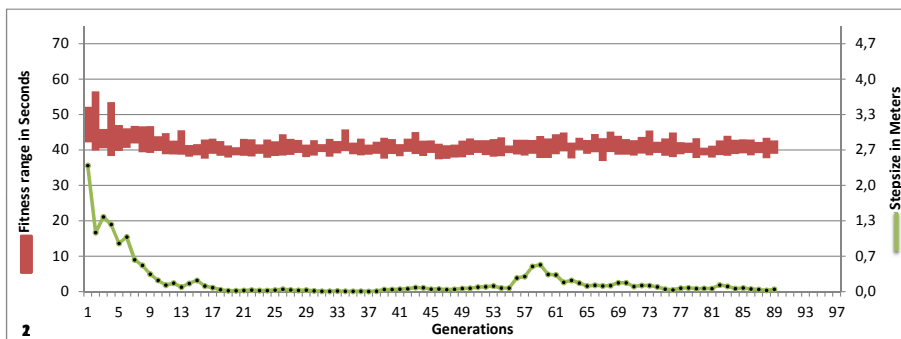


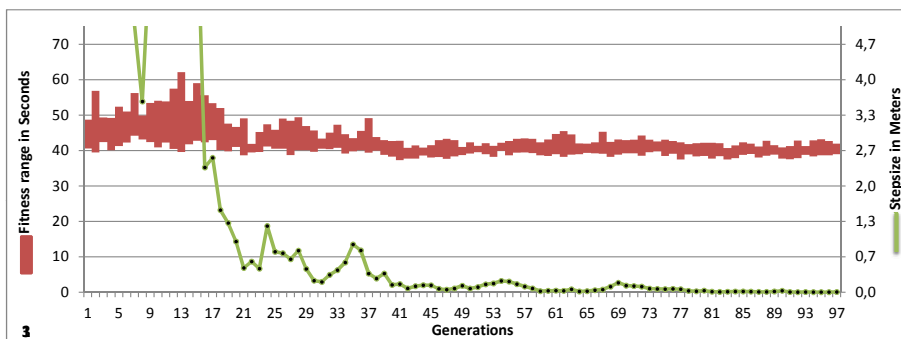
Figure 6.3: Comparison of the average efficiency for the 3 expert environments and the 3 environments found by the Evolutionary Strategy for the Corridor experiment



(a) ES I1



(b) ES I2



(c) ES I3

Figure 6.4: Progression of Evolutionary strategy for the Intersection experiment. Pedestrian range is from the child with the best fitness to the child with the worst fitness of that generation.

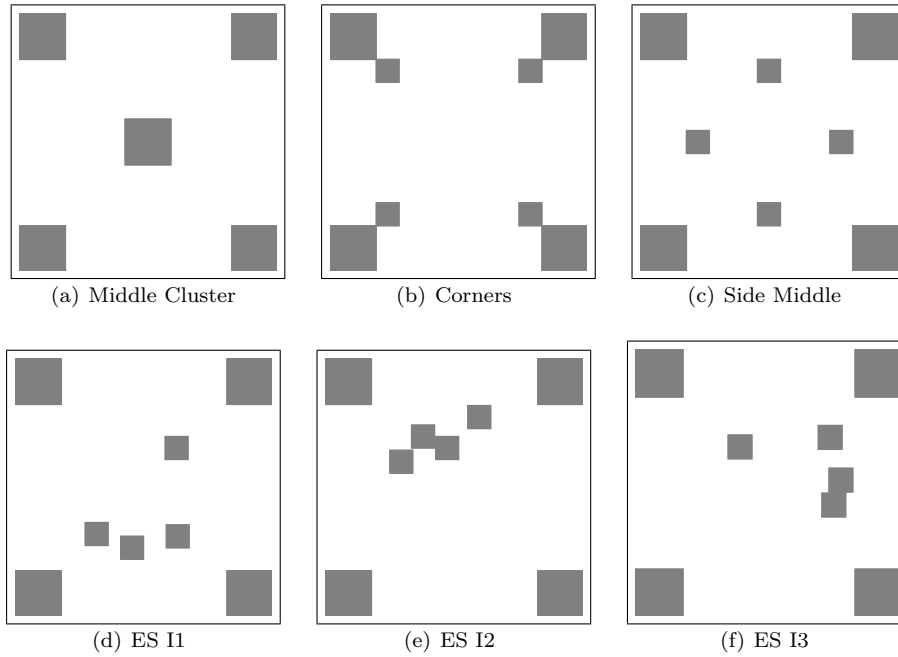


Figure 6.5: Visual representation of the 3 expert Intersection environments on the first row and 3 environments found by the Evolutionary Strategy on the second row

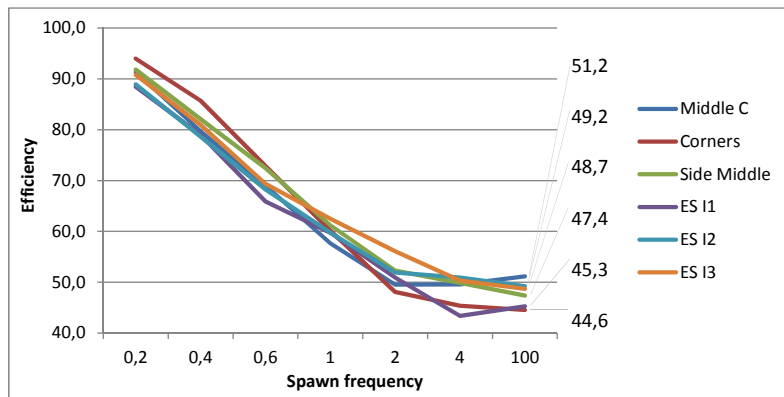


Figure 6.6: Comparison of the average efficiency for the 3 expert environments and the 3 environments found by the Evolutionary Strategy for the Intersection experiment

Chapter 7

Discussion

In this chapter the results found by the experiments are discussed. First the simulator validation experiment is discussed. This is followed by a discussion of the Corridor and Intersection experiments.

7.1 Simulator

When looking at the findings (Appendix A) the clogging effect is very much present in the simulations. The clogging effect is known to emerge commonly with simulators based on the social forces model.

Lane formation also occurs readily as seen with pedestrians[15]. The number of agents that make up a lane also seems to concur with that observed amongst pedestrians. Finally, the time one particular lane survives is also limited to 10-20 seconds. Compared to the simulators described in 1.1 lane formation in the simulator has lane lengths and durations that match that what is seen among pedestrians more accurately.

The circulation flows however did not seem to develop. Some imbalances were seen in the form of asymmetry, but not a clear rotation. These flows do, however, not commonly occur among pedestrians, and are subject to the environment. Their absence could be the result of testing in the wrong environment. However another explanation could be that the simulator does not represent pedestrian behaviour well enough for the circular flows to occur.

7.2 Evolutionary Strategy

When looking at the ES runs for the corridor experiment it shows that although the noise described in 4.3 is present, the resampling appears to work in that it provides the ES with a fitness landscape that has a level of noise where useful discrimination between solutions is still possible. Both stepsizes and fitness ranges decrease over time. This indicated that convergence is taking place.

When comparing this to the runs for the intersection experiment the same convergence is not seen. In the intersection runs the stepsize does decrease over time, but the solutions found do not seem to improve by much. Also, the fitness range within one generation, although fluctuating, remains small and does not seem to decrease over time. This could be because the pedestrian density is not high enough or because the simulator does not seem to reproduce the circular flows behaviour. A possible explanation why the density can influence convergence is that with a low density, the differences in fitness between the solutions are very low. The lack of circulating flows could contribute to this issue in a similar fashion. When circulating flows occur amongst pedestrians, they increase their efficiency. If this were to also happen in the simulator, the result would be an increase in fitness range.

The best solutions found in the 3 runs for the corridor experiment note a remarkable result. All solutions have a better average pedestrian efficiency than an empty corridor at high densities. When looking at lower densities, the empty corridor performs best. This can be explained by obstacles initially resulting in a detour, but as density increases, also start to contribute to more efficient pedestrian formations. At high density the increase in pedestrian formation outweighs the forced detour, thus causing a net increase in pedestrian efficiency. An example of this can be seen in 6.4. The box plots in Appendix B show that it is unlikely that the measured fitness difference is noise. The results of the best solutions found in the 3 runs for the intersection experiment do not show any significant gain over the 3 expert environments. Furthermore, the contrast between the 3 expert environments seems to be very low as well. In the lower density ranges, ES I3 is slightly better than the 5 other solutions, but given that these environments were found when optimizing for a spawn frequency of 100, these results could be due to chance. The box plots in C also show not being able to differentiate between the environments on most density levels.

Chapter 8

Conclusions

Going back to the first research questions, does the pedestrian simulator produce realistic behaviour? The simulator is tested for three known emergent pedestrian behaviours and no evidence was found that would suggest that the simulator does not simulate realistic behaviour.

Our second research question is, can a pedestrian simulator be used as a fitness function for an Evolutionary Strategy? From the corridor experiment it can be concluded that this is the case. Although the simulator generates a noisy landscape, at high density, solutions can be discriminated correctly and convergence takes place.

The last research question is, can an Evolutionary Strategy find better solutions than experts? In the corridor experiment, all runs produced a better solution at high density than the best expert solution. This is the most promising result of this research as it not only shows that placing obstacles in pedestrian areas can lead to an increased pedestrian efficiency but also suggests that the location and size can be found by an Evolutionary Strategy.

8.1 Future research

Injury: Currently the simulator measures agent walking times. A very interesting extension would be measuring injury rate as a result of pressure. Although very little is known how pedestrians get injured when in dense crowds, it does happen when inter-pedestrian pressure rises. [16].

Pedestrian Compressibility: Pedestrians are not static in their shape. They are to some extent compressible. Including compressibility of agents as done by [30] would contribute to a more realistic model and supply extra tools to measure pedestrian injury rate.

OCEAN Model: In crowd simulation there has been a focus on crowd cognition and understandings while emotions and the phenomenology of crowd

participation has been largely ignored. [27]. In the last couple of years, there have been a few attempt to focus more on those other topics [25] [9], however, none of these studies are based on empirical evidence that certain emotions effect pedestrian behaviour. A model based on empirically observed correlations between personality traits and pedestrian behaviour would be adding more realistic and accurate pedestrian behaviour.

Circular Flows: Circular flows have not been observed in the simulator. Further understanding and reproducing this emergent behaviour would increase the validity of the simulator.

Further Parallelization: It is possible to parallelize the evaluation of one child by implementing a parallel social forces model as suggested by [26]. This would make running simulations with a higher density feasible.

CMA ES: A basic Evolutionary strategy has been used. Replacing this with a CMA_ES could better the results since it is particularly well suited for a noisy fitness landscape.

Chapter 9

Acknowledgements

I would like to thank my supervisor Prof. Thomas Bäck for his help, enthusiasm and inspiration, and my second supervisor Michael Emmerich, PhD. I would also like to thank Cees. A. Swenne, PhD, for critically reading the manuscript of my thesis, and Jonathan. K. Vis, MSc, and Jan. N. van Rijn, BSc, for their valuable criticisms and suggestions.

Appendix A

Emergent Behaviour

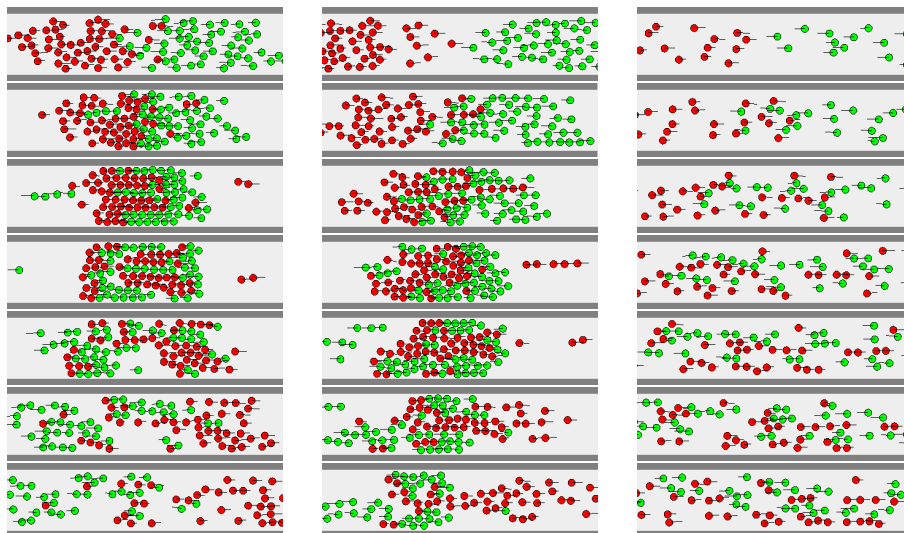


Figure A.1: Timeseries on Lane formation emergent behaviour for spawn frequencies 100, 4 and 1Hz (from left to right) and for timestamps 8,13,18,23,28,33 and 38 (from top to bottom)

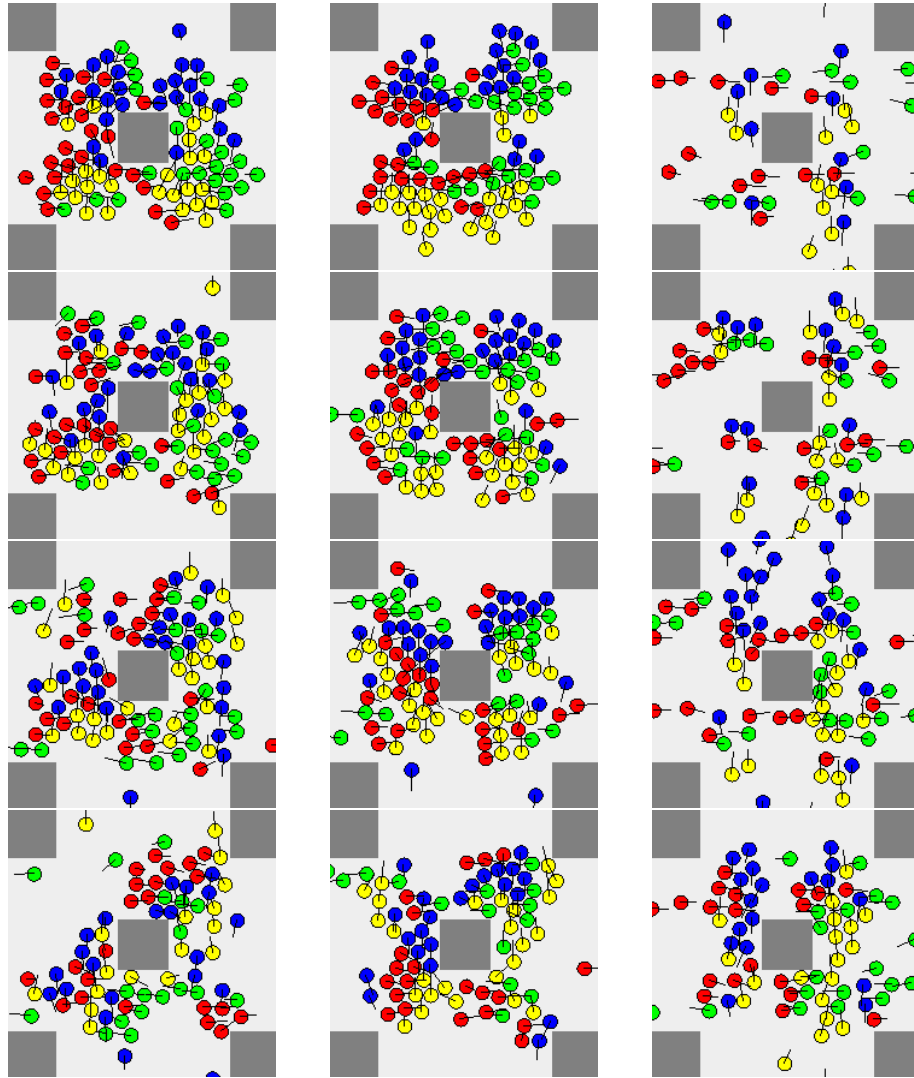


Figure A.2: Timeseries on Circular emergent behaviour for spawn frequencies 100, 4 and 1 (from left to right) and for timestamps 5,10,15 and 20 (from top to bottom)

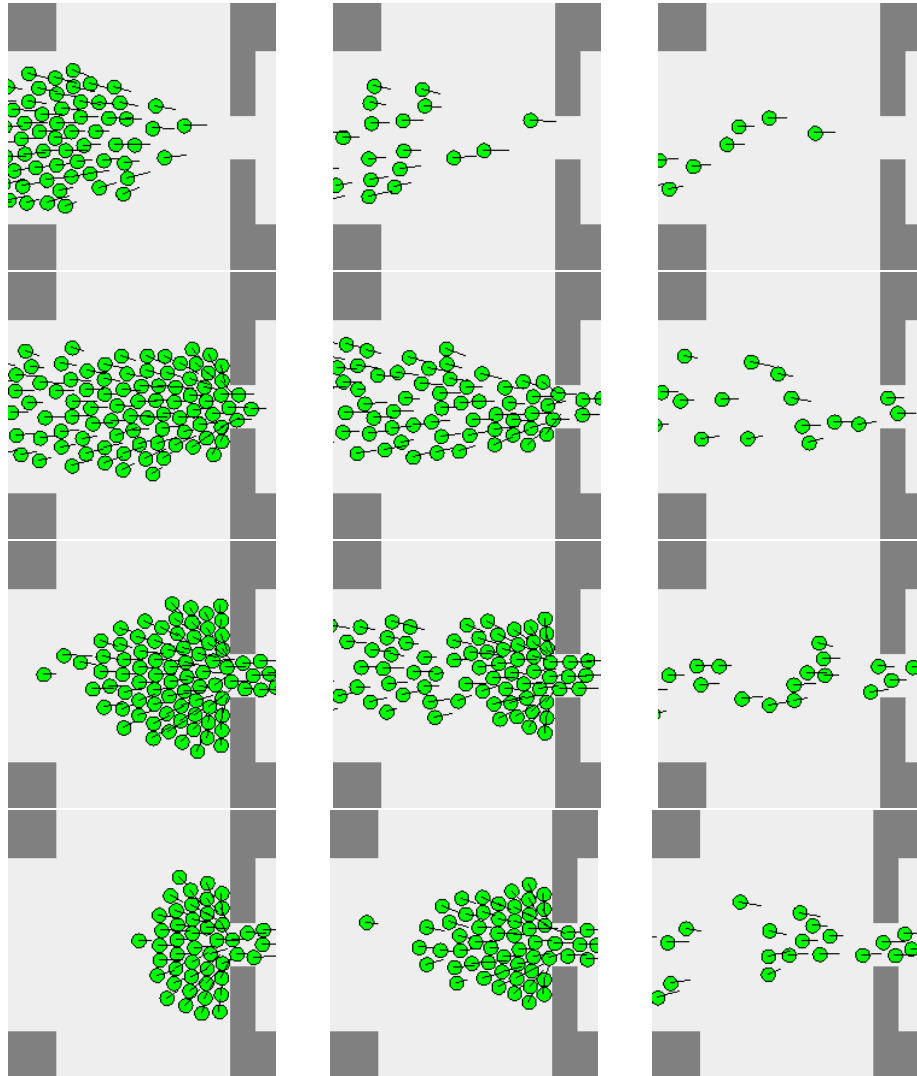


Figure A.3: Timeseries on Clogging emergent behaviour for spawn frequencies 100, 4 and 1 (from left to right) and for timestamps 8,13,18 and 23 (from top to bottom)

Appendix B

Corridor Results

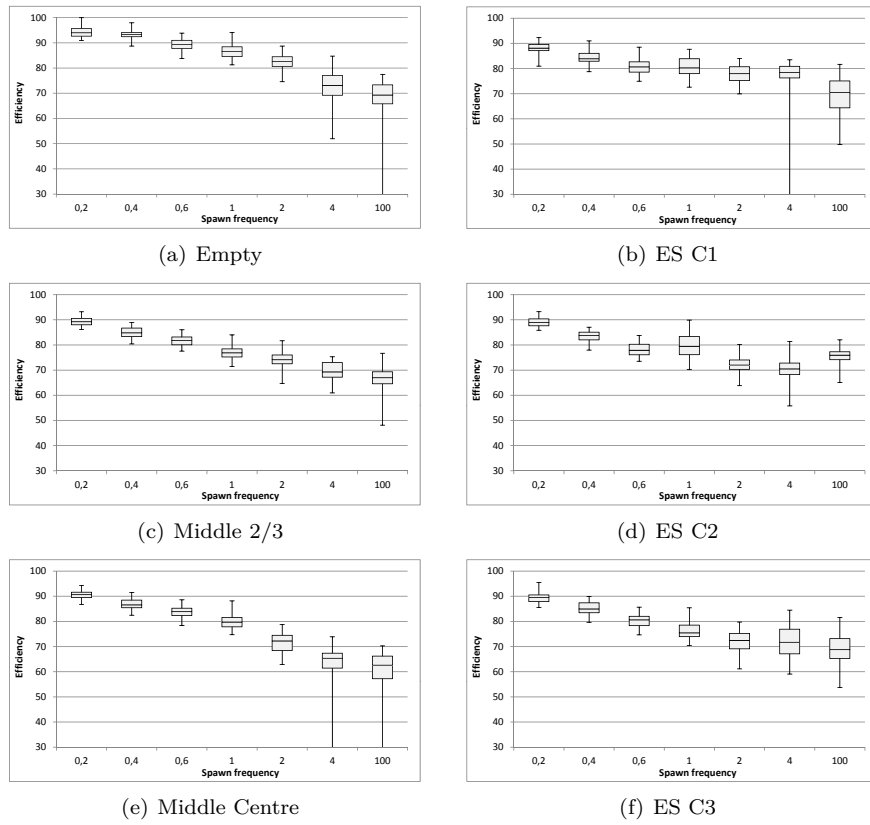
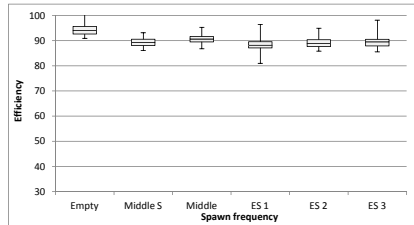
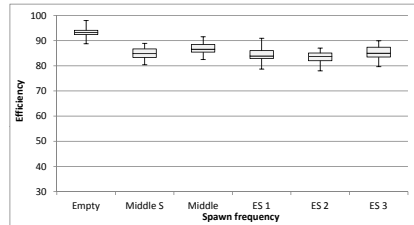


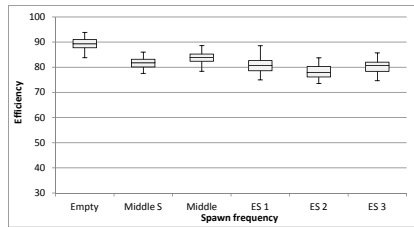
Figure B.1: Pedestrian efficiency against pedestrian density for the Corridor environments. 3 expert solutions on the left and 3 solutions found by the evolutionary strategy on the right



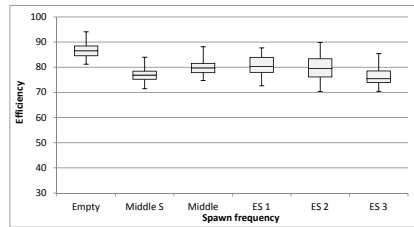
(a) 0.2



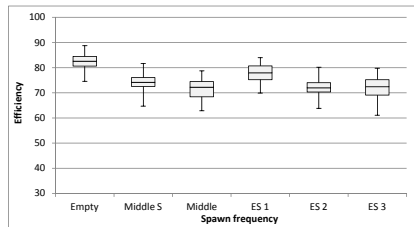
(b) 0.4



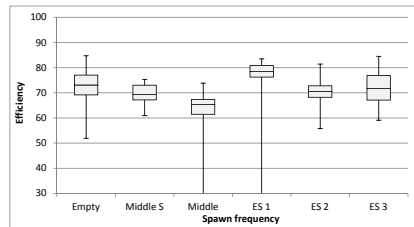
(c) 0.6



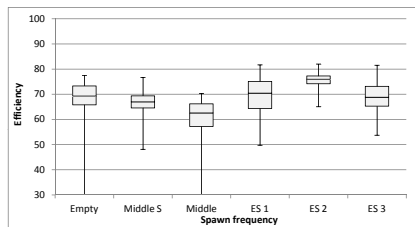
(d) 1



(e) 2



(f) 4



(g) 100

Figure B.2: Pedestrian efficiency in the Corridor environments for environments Empty, Middle 2/3, Middle Centre, ES C1, ES C2 and ES C3 environments for different densities

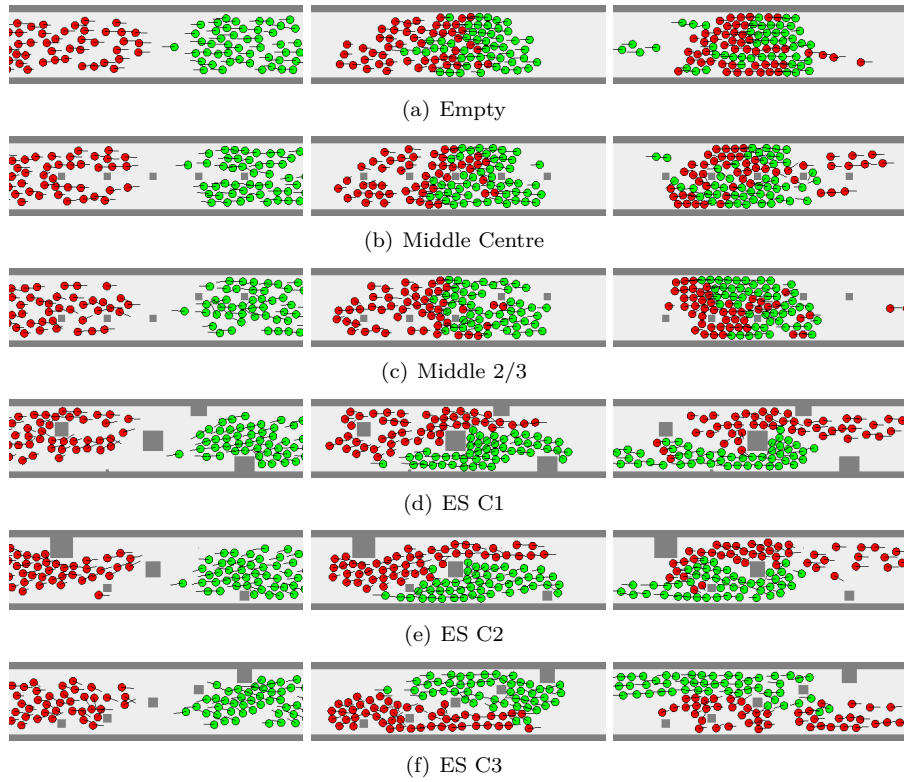
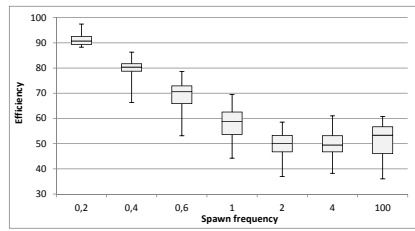


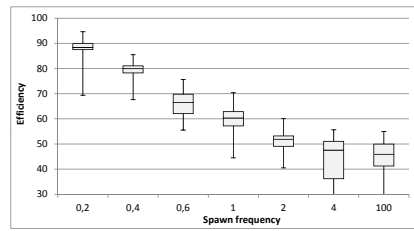
Figure B.3: Timeseries of the 3 Evolutionary Strategy Corridor environments and 3 expert environments during the fitness function for timestamps 10, 20 and 30 from left to right.

Appendix C

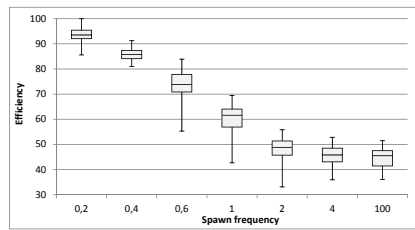
Intersection Results



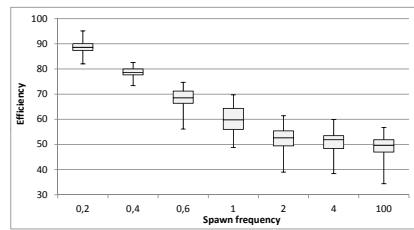
(a) Middle Cluster



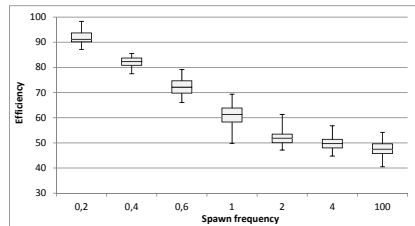
(b) ES C1



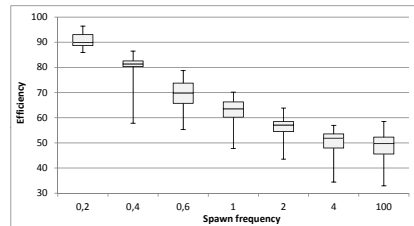
(c) Corners



(d) ES C2

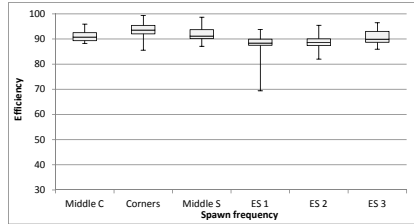


(e) Side Middle

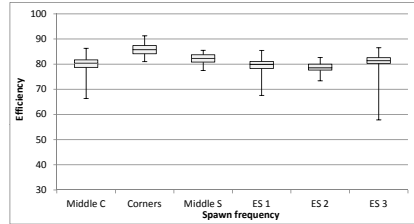


(f) ES C3

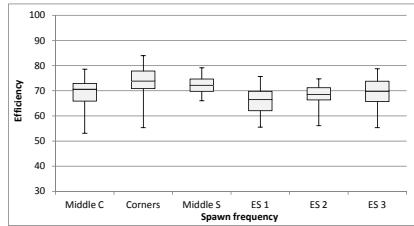
Figure C.1: Pedestrian efficiency for Intersection pedestrian density. Middle Cluster, Corners, Side Middle environments on the left and ES I1, ES I2 and ES I3 environments on the right



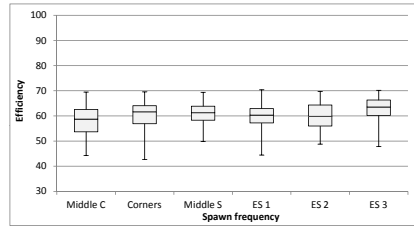
(a) 0.2



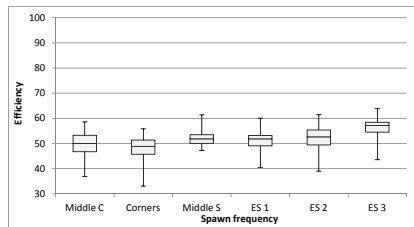
(b) 0.4



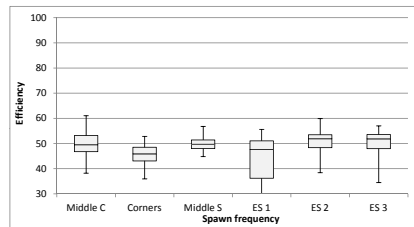
(c) 0.6



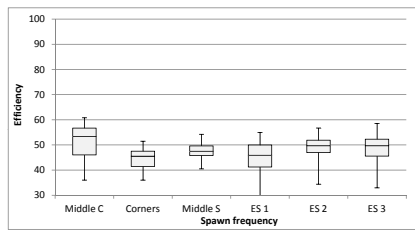
(d) 1



(e) 2



(f) 4



(g) 100

Figure C.2: Pedestrian efficiency for Intersection environments Middle Cluster, Corners, Side Middle, ES I1, ES I2 and ES I3 environments for different densities

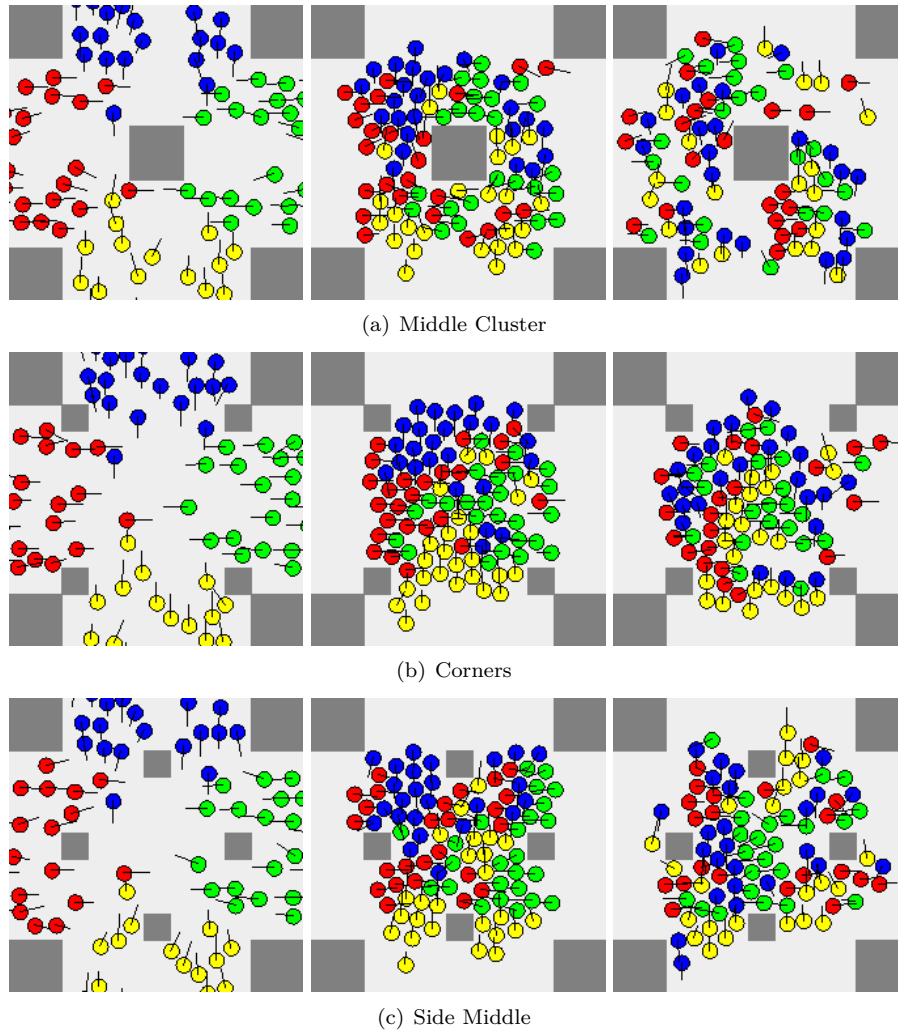


Figure C.3: Timeseries of the 3 Evolutionary Strategy Intersection environments during the fitness function for timestamps 10, 20 and 30 from left to right.

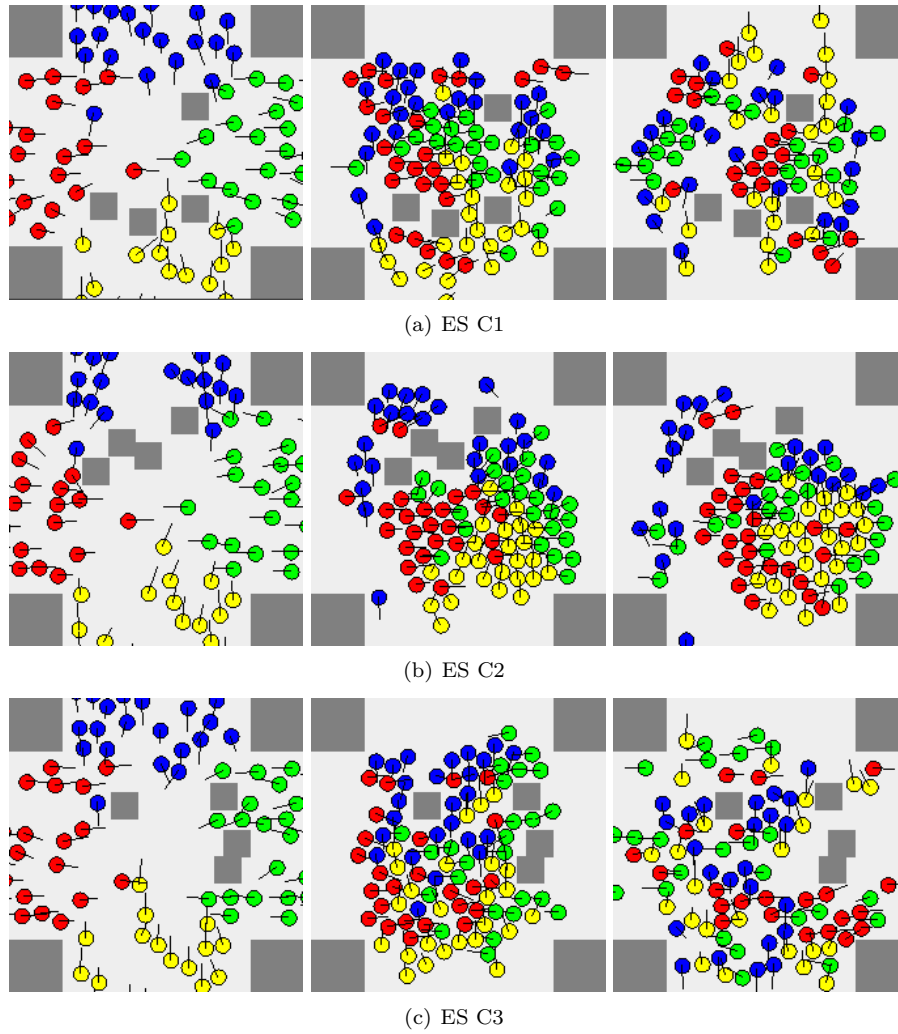


Figure C.4: Timeseries of the 3 expert Intersection environments during the fitness function for timestamps 10, 20, and 30 from left to right.

Bibliography

- [1] J. Averill. Five Grand Challenges in Pedestrian and Evacuation Dynamics. In *5th International Conference on Pedestrian and Evacuation Dynamics*, pages 1–11. Springer US, 2010.
- [2] Th. Bäck. *Evolutionary Algorithms in Theory and Practice*. Oxford University Press, Oxford, UK, 1996.
- [3] D. Bauer. Comparing pedestrian movement simulation models for a crossing area based on real world data. In *5th International Conference on Pedestrian and Evacuation Dynamics*, pages 547–556. Springer US, 2010.
- [4] National Research Council (U.S.). Transportation Research Board. Highway capacity manual, special report 209. *Transportation Research Board, National Research Council*, 1985.
- [5] C. Burstedde, K. Klauck, A. Schadschneider, and J. Zittartz. Simulation of pedestrian dynamics using a two-dimensional cellular automaton. In *Physica A: Statistical Mechanics and its Applications*, volume 295, pages 507–525. Elsevier, 2001.
- [6] W. Daamen and S. Hoogendoorn. Experimental Research of Pedestrian Walking Behavior. *Transportation Research Record: Journal of the Transportation Research Board*, 1828:20–30, 2003.
- [7] W. Daamen and S. Hoogendoorn. Free speed distributions for pedestrian traffic. In *Transportation Research Board 85th Annual Meeting Compendium of Papers*, pages 1–13. Transportation Research Board of the National Academies, 2006.
- [8] J. Drury, C. Cocking, and S. Reicher. Everyone for themselves? a comparative study of crowd solidarity among emergency survivors. *British Journal of Social Psychology*, 48(3):487–506, 2009.
- [9] F. Durupinar, J. Allbeck, N. Pelechano, and N. Badler. Creating crowd variation with the ocean personality model. In *Proceedings of the 7th international joint conference on Autonomous agents and multiagent systems - Volume 3, AAMAS '08*, pages 1217–1220, Richland, SC, 2008. International Foundation for Autonomous Agents and Multiagent Systems.

- [10] R. Fahy and G. Proulx. ‘Panic’ and human behaviour in fire. In *Proceedings of the 4th International Symposium on Human Behaviour in Fire*, pages 387–398. Interscience Communications, 2009.
- [11] P. G. Gipps and B. Marksjo. A micro-simulation model for pedestrian flows. *Mathematics and Computers in Simulation*, 27:95–105, 1985.
- [12] E. Goffman. *Relations In Public: Microstudies In The Public Order*. Basic Books, 1971.
- [13] S. Guy, J. Chhugani, S. Curtis, P. Dubey, M. Lin, and D. Manocha. Pedestrians: a least-effort approach to crowd simulation. In *Proceedings of the 2010 ACM SIGGRAPH/Eurographics Symposium on Computer Animation*, SCA ’10, pages 119–128. Eurographics Association, 2010.
- [14] N. Hansen and A. Ostermeier. Completely Derandomized Self-Adaptation in Evolution Strategies. *Evolutionary Computation*, 9(2):159–195, 2001.
- [15] D. Helbing, L. Buzna, A. Johansson, and T. Werner. Self-organized pedestrian crowd dynamics: Experiments, simulations, and design solutions. *Transportation Science*, 39(1):1–24, 2005.
- [16] D Helbing, A Johansson, and H. Z. Al-Abideen. The dynamics of crowd disasters: An empirical study. *Physical Review E*, 75:046–109, 2007.
- [17] D. Helbing and P. Molnár. Social force model for pedestrian dynamics. *Physical Review E*, 51(5):4282–4286, 1995.
- [18] I. Karamouzas, R. Geraerts, and M. Overmars. Indicative routes for path planning and crowd simulation. In *FDG ’09: Proceedings of the 4th International Conference on Foundations of Digital Games*, pages 113–120. ACM, 2009.
- [19] A. Kirchner and A. Schadschneider. Simulation of evacuation processes using a bionics-inspired cellular automaton model for pedestrian dynamics. *Physica A*, 312(1-2):260–276, 2002.
- [20] J. W. Kruisselbrink. *Evolution Strategies for Robust Optimization*. PhD thesis, Universiteit Leiden, 2012.
- [21] S. M. LaValle. *Planning Algorithms*. Cambridge University Press, 2006. Available at <http://planning.cs.uiuc.edu/>.
- [22] B. Liebowitz. Human territories: How we behave in space-time. *Family Process*, 15(4):447–451, 1976.
- [23] S. Okazaki. Movement in architectural space, part 1: Pedestrian movement by the application on of magnetic models. In *Transactions of the Architectural Institute of Japan*, volume 283, pages 111–119, 1979.

- [24] J. Ondřej, J. Pettré, A. Olivier, and S. Donikian. A synthetic-vision based steering approach for crowd simulation. In *ACM Transactions on Graphics*, volume 29, pages 123:1–123:9. ACM, 2010.
- [25] N. Pelechano, J. M. Allbeck, and N. I. Badler. Controlling individual agents in high-density crowd simulation. In *SCA '07: Proceedings of the 2007 ACM SIGGRAPH/Eurographics symposium on Computer animation*, pages 99–108. Eurographics Association, 2007.
- [26] M. Quinn, R. Metoyer, and K. Hunter-Zaworski. Parallel implementation of the social forces model. In *Proceedings of the Second International Conference in Pedestrian and Evacuation Dynamics*, pages 63–74, 2003.
- [27] S. Reicher. The psychology of crowd dynamics. *Blackwell handbook of social psychology: Group Processes*, 2001.
- [28] T. Rupperecht, W. Klingsch, and A. Seyfried. Influence of geometry parameters on pedestrian flow through bottleneck. In *5th International Conference on Pedestrian and Evacuation Dynamics*, pages 71–80. Springer US, 2010.
- [29] M. Swenne and Th. Bäck. Optimizing pedestrian environments with evolutionary strategies. In *6th International Conference on Pedestrian and Evacuation Dynamics*. Springer, 2012.
- [30] J. Wąs, J. Myśliwiec, and R. Lubaś. Towards realistic modeling of crowd compressibility. pages 527–534. Springer US, 2010.
- [31] D. Yanagisawa, A. Kimura, A. Tomoeda, R. Nishi, Y. Suma, K. Ohtsuka, and K. Nishinari. Introduction of frictional and turning function for pedestrian outflow with an obstacle. *Physical Review E*, 80:036–110, 2009.
- [32] I. Zeiler, C. Rudloff, and D. Bauer. Modelling random taste variations on level changes in passenger route choice in a public transport station. In *5th International Conference on Pedestrian and Evacuation Dynamics*, pages 185–195. Springer US, 2010.